A NOVEL MECHANICAL TRANSMISSION APPLIED TO PERCUTANEOUS RENAL ACCESS

Dan Stoianovici, Ph.D.[1,2], Jeffrey A. Cadeddu, M.D.[1], Roger D. Demaree[4], Stephen A. Basile, Sc.D.[4], Russell H. Taylor Ph.D.[3], Louis L. Whitcomb, Ph.D.[2], William N. Sharpe, Jr., Ph.D.[2], and Louis R. Kavoussi, M.D[1].

[1]The James Buchanan Brady Urological Institute, The Johns Hopkins Medical Institutions.
[2]Department of Mechanical Engineering , The Whiting School of Engineering, The Johns Hopkins University.
[3]Department of Computer Science, The Whiting School of Engineering, The Johns Hopkins University.
[4]Applied Physics Laboratory, The Johns Hopkins University.

Conference Topic: Methods and Instrumentation
Clinical Biomechanics

Keywords: radiological guidance, percutaneous access, robot registration, friction transmission

Corresponding Address: Dan Stoianovici, Ph.D.
Director, Robotics Division
Brady Urological Institute, A344
The Johns Hopkins University
4940 Eastern Avenue
Baltimore, Maryland 21224

e-mail: dss@spray.me.jhu.edu
Phone: 410-550-0403
Fax: 410-550-3341
Beeper: 410-283-4398

.

ABSTRACT

This paper presents a radiological guidance method and robotic system designed to facilitate renal surgical procedures. Combines the guidance procedure normally employed by practicing surgeons with a simple and cost-effective needle injection device. The needle injector exhibits an extremely low radiological profile while providing actuated needle motion. The system can be easily utilized by urologic surgeons and can be readily adaptable to any operating room.

1. INTRODUCTION

As an alternative to traditional open surgery, percutaneous surgery significantly reduce patient morbidity and recovery time. However, percutaneous needle access can be challenging and requires extensive clinical experience due to the lack of three-dimensional information provided to the surgeon by current standard inter-operative imaging techniques.

To overcome this problem several groups have proposed robotic systems to assist in needle placement. Potamianos and Davies [1,2] use a stereo-pair of two x-ray views registered to a common fiducial system with a 5DOF passive linkage equipped with position encoders to position a passive needle guide. Bzostek et al [3] propose an active robot for similar purposes. Although these systems successfully address issues of image-to-robot registration and provide convenient means for defining target anatomy, in their present state of development these robotic systems are expensive and cumbersome for practical use in the operating room. Further, at least for the current implementation of [3], the radiological profile of the end-effector may interfere with a clear view of the anatomic target.

Our goal was to develop a system to improve the accuracy and precision during percutaneous renal access. To achieve this we focused on: (1) needle placement accuracy, (2) procedure duration, (3) patient safety, (4) sterility, and (5) surgeon radiation exposure. After extensive observations of surgeons performing needle insertion, we developed a mechanical system that mimics and improves upon the surgeon's standard technique. The key advantages of this approach are that it employs a proven radiological needle alignment procedure, improves accuracy in comparison to purely manual placement, and enables lateral fluoroscopic monitoring of the needle *without* necessitating computer-based vision.

Percutaneous renal access procedures are often performed in radiology suites where sophisticated imaging devices are available. Performing the renal access in the operating room (OR) significantly reduces cost, decreases patient morbidity, and allows the surgeon to have full control over the entire procedure. The imaging commonly available in the OR is uni-planar fluoroscopy provided by a "C-arm". An inexpensive robotic system for the OR utilizing existing C-arm imagery would be widely and immediately deployable.

2. SUPERIMPOSED NEEDLE REGISTRATION

Manual renal access traditionally proceeds with the surgeon positioning the C-arm over the collecting system and choosing the target calyx and the skin insertion site. The fluoroscope is then positioned to align the desired needle entry point and the target so that they are superimposed in the image. This alignment defines the needle trajectory and is memorized by the locked orientation of the C-arm. The needle, the entry point, and the target are manually aligned so that they are superimposed as a single point on the fluoroscopic image. The surgeon manually inserts the needle, while trying to maintain fluoroscopic alignment. However, needle deflection and shifts in position can alter final needle location. Furthermore, a lateral view is not simultaneously available because fluoroscope is used to maintain axial needle alignment. In consequence, no needle depth imagery is available. Thus, appropriate needle placement is highly dependent upon the surgeon's experience, as well as trial and error.

We developed a system that mimics while facilitating this surgical technique. The C-arm and needle are aligned as above. The needle axis is then mechanically locked on the desired line of insertion by a passive robotic arm. In this way the insertion line is memorized by the locked position of the arm, enabling the surgeon to rotate the C-arm and obtain a lateral view. The insertion depth and needle path can then be directly monitored while the device maintains the needle trajectory. Note that the method only requires direct observation by the surgeon, and does not require continuous manual alignment. Direct observation of the insertion depth allows the surgeon to compensate for the soft tissue deflection of the kidney and surrounding tissue. Thus, this system can potentially significantly reduce operative time and expense while improving both safety and accuracy.

Note that, the proposed method does not require image correction and calibration. By superimposing the needle, the entry point, and the target, the image distortions are identical and, therefore, they are relatively zero. Furthermore, the method only requires direct observation by the surgeon, and does *not require* computer-based image processing.

3. THE NEEDLE INJECTOR

Superimposed registration requires a radio-lucent needle holder to provide unimpeded needle alignment without obstructing the fluoroscopic image of the target calyx. An active needle insertion mechanism incorporated in this holder would reduce the surgeon's radiation exposure and increase accuracy. Furthermore, grasping the barrel of the needle, not the needle head, would significantly reduce the unsupported length of the needle during insertion, thus minimizing the lateral flexure of the needle under insertion loading. Therefore, we sought to develop an injector that: 1) is radio-lucent, 2) actively drives the needle, and 3) grasps the needle barrel. After several iterations of possible mechanical transmission designs to meet these requirements, we converged to on a design based on a novel mechanical transmission, "The R-T Friction Transmission with Axial Loading".

3.1. The R-T Friction Transmission with Axial Loading; Principle:

Rotational to translational (R-T) friction transmissions are known since ancient eras. As a common characteristic of all such designs, the force generating the friction was oriented radial with respect to the rotational shaft of the transmission. Our approach differs in this orientation of the friction's normal force axial with respect to the rotational shaft of the transmission. This axial loading can be significantly larger than the commonly used radial loading at similar sizes, yielding to increased force and power transmission. Furthermore, the axial loading involves a simpler mechanical designs and allows miniaturization.

The isometric schematic in Fig. 1a illustrates the principle of transmission. This non-backlash transmission converts the rotational motion (R) of the shaft (6) into the translation (T) of the shaft (4) or vice-versa. The output shaft (4) is squeezed between the disks (6, 3) generating the transmission friction. The bushings (1), (2), (5), and (7) are grounded maintaining the relative position of the shafts.

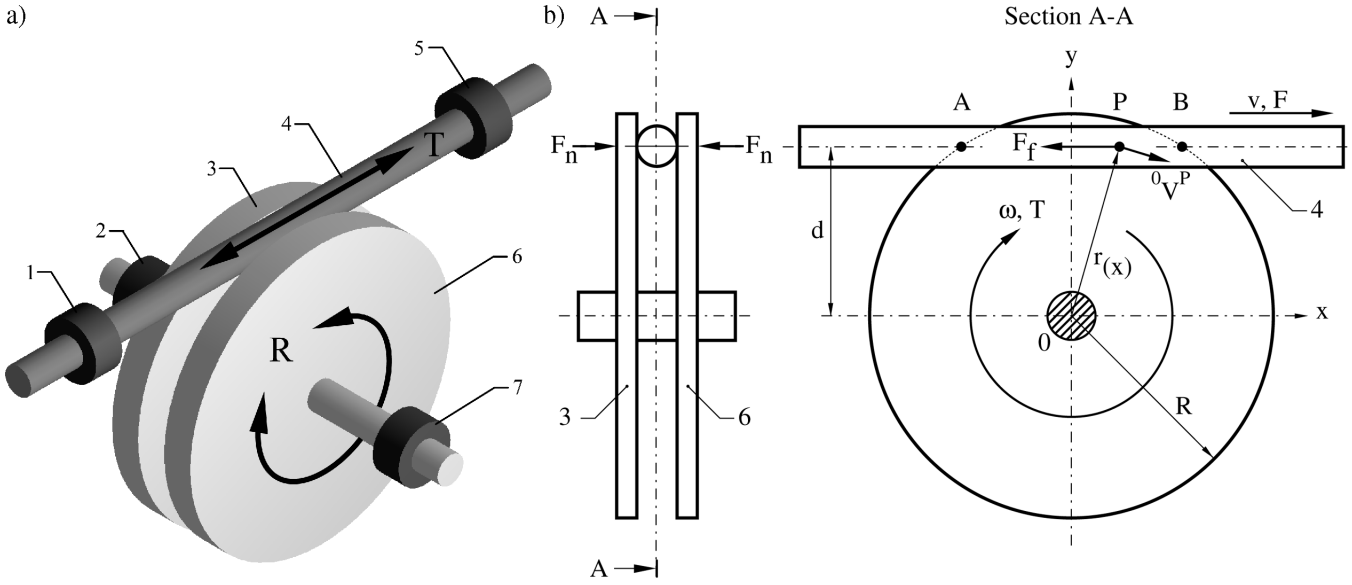

Figure 1. Friction transmission with axial loading: a) Principle of operation, b) Kinematics

The kinematics is illustrated in Fig. 1b. The disks (3) and (6) are axially loaded with the force $\mathbf{F_n}$ generating the friction force of the transmission $\mathbf{F_f} = \mu \mathbf{F_n}$. Here, μ is the Coulomb coefficient of friction between the disks (3, 6) and the output shaft (4). The output force of the transmission F is bounded by $2\,\mathbf{F_f}$, ($\mathbf{F} \le 2\mathbf{F_f}$), therefore, the transmission slips when overloaded. Theoretically, the friction force acts on the contact line AB, on both disks. Consider a planar Newtonian system of coordinates **x0y** centered in the axis of the input shaft (see Fig. 1b). The absolute velocity (with respect to 0) of a contact point P of the disk is:

$$^0\mathbf{V^P} = \omega\, \mathbf{r_{(x)}} \qquad \text{(Eq. 1)}$$

where, ω is the angular velocity of the input shaft (3, 6) and $\mathbf{r_{(x)}}$ is the position vector of the point P. The $\mathbf{x}$ and $\mathbf{y}$ components of this velocity may be calculated as:

$$\begin{cases} {}^{0}\mathbf{V_x^P} = \omega \mathbf{d} \\ {}^{0}\mathbf{V_y^P} = -\omega \mathbf{x} \end{cases} \quad \text{(Eq. 2)}$$

where, $\mathbf{d}$ is the distance between the input and output shaft axes, and the coordinate x defines the position of the point P on the line AB. In these equations one may observe that ${}^{0}\mathbf{V_x^P}$ is constant along the line AB and ${}^{0}\mathbf{V_y^P}$ is linearly dependent on $\mathbf{x}$. The first equation defines the kinematic transfer function of the transmission as:

$$\mathbf{V} = \omega \mathbf{d} \quad \text{(Eq. 3)}$$

where, $\mathbf{V}$ is the velocity of the output, ω is the angular velocity of the input, and the design parameter $\mathbf{d}$ defines the velocity gain. Similarly, the dynamic transfer function of the transmission may be calculated as:

$$\mathbf{F} = \frac{\mathbf{T}}{\mathbf{d}}; \qquad \mathbf{F} \le 2\mu \mathbf{F_n} \quad \text{(Eq. 4)}$$

where, $\mathbf{T}$ is the input torque and $\mathbf{F}$ is the output force.

The transmission dissipates mechanical power due to the y-directional sliding friction of the disks (3,6) with respect to the output shaft (4) on the contact line AB. The velocity of a point P of the disk relative to the output shaft (4) (when the transmission is under-loaded $\mathbf{F} \le 2\mu \mathbf{F_n}$), is given by:

$$\begin{cases} {}^{4}\mathbf{V_x^P} = 0 \\ {}^{4}\mathbf{V_y^P} = -\omega \mathbf{x} \end{cases} \quad \text{(Eq. 5)}$$

This shows that there is no energy loss due to the x-directional friction, however, the y-directional friction component exhibits mechanical work. The lost ($\mathbf{W_l}$) and transmitted ($\mathbf{W_t}$) power of the transmission may be calculated using the Coulomb friction model as:

$$\begin{cases} \mathbf{W_l} = \dfrac{4}{2\mathbf{l}} \displaystyle\int_0^{\mathbf{l}} \mathbf{F_f}\ {}^{4}\mathbf{V_y^P}\, \mathbf{dx} = -\mu \mathbf{F_n}\, \omega \mathbf{l} \\ \mathbf{W_t} = 2\,\mathbf{F_f}\ {}^{4}\mathbf{V_y^P} = 2\mu \mathbf{F_n}\, \omega \mathbf{d} \end{cases} \quad \text{(Eq. 6)}$$

where, $\mathbf{l} = \dfrac{|\mathbf{AB}|}{2} = \sqrt{\mathbf{R}^2 - \mathbf{d}^2}$ with $\mathbf{R}$ the radius of the disks (3, 6), maximum loading $\mathbf{F} = 2\mu \mathbf{F_n}$ of the transmission was considered, and the static and dynamic coefficients of friction μ were considered equal (most disadvantageous case). Consequently, the peek power efficiency of the transmission may be calculated as:

$$\varepsilon_{(\mathbf{d})} = \frac{\mathbf{W_t}}{\mathbf{W_t} - \mathbf{W_l}} = \frac{2\mathbf{d}}{2\mathbf{d} + \mathbf{l}} \quad \text{(Eq. 7)}$$

We note here that the efficiency depends only on the ratio of $\mathbf{d}$ to $\mathbf{R}$. In this calculation the friction encountered in the supporting bushings has been neglected. Defining this ratio as:

$$\mathbf{f} \equiv \frac{\mathbf{d}}{\mathbf{R}} \quad \text{(Eq. 7)}$$

the efficiency of the transmission becomes:

$$\varepsilon_{(\mathbf{f})} = \frac{2\mathbf{f}}{2\mathbf{f} + \sqrt{1 - \mathbf{f}^2}} \qquad \text{(Eq. 8)}$$

This dependence of the transmission efficiency on the position of the output with respect to the input shafts is graphically represented in Fig 2.

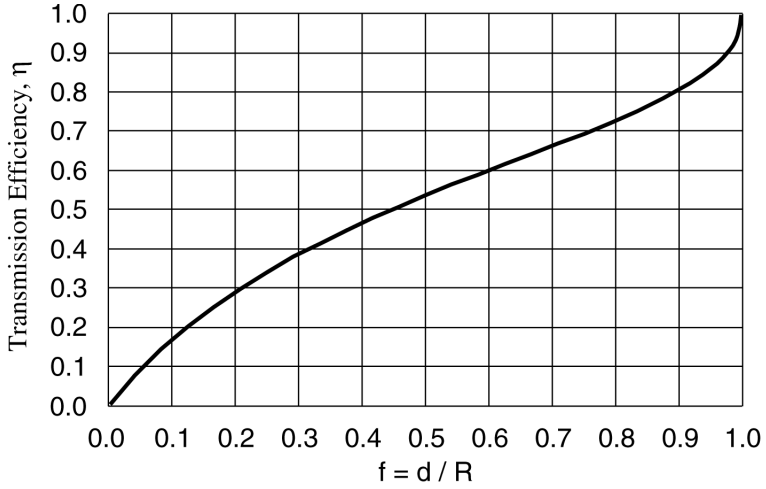

Figure 2. The peek power efficiency of the transmission

The extremes of the graph show that the output power is 0 if $\mathbf{d} = 0$ and no power is lost if $\mathbf{d} = \mathbf{R}$. As a design prescription, the graph concludes that the dimension **d** should be set as close to **R** as possible, in order to maximize the efficiency of the transmission.

Note that a rotational motion may also be imposed over the translation of the output shaft (4) by either using different materials (i.e. different coefficients of friction) for the disks (3) and (6) or by slightly inclining the axis of the output shaft (4) with respect to the axis of the disks (3, 6) in **y** direction (see Fig. 1a).

3.2. PAKY: A Radio-Lucent Needle Driver:

Based on this novel transmission we designed a driver of an 18 gauge trocar-needle to be used for percutaneous access of the kidney, the PAKY needle driver. The driver assembly is presented in Fig. 3. The trocar needle (1) is used as the output shaft of the transmission (2). The input shaft of the transmission is driven from a variable speed DC motor located in a housing (3). The transmission (2) is mounted in the housing (3) by using a ball-lock.

An exploded view of the transmission assembly is represented in Fig. 4a. The housing of the transmission (1) is constructed of acrylic in order to be radio-lucent. It presents a rimmed hole that the input shaft (2) and the axial-loading bushing (3) slide into. This hole accounts for the bushings (2) and (7) of Fig. 1. One more rimmed hole, normal and internally tangent to the previous hole is used for the orientation of the needle (6). This accounts for the bushings (1) and (5) of Fig. 1. The input shaft (2) is also constructed of acrylic. A small slot at one end of the shaft couples the motor while the other end is threaded in order to assemble with the nut (5). The bushing (3) slides over the shaft (2) and is axially loaded through the O-ring (4) with the nut (5). The bushing (3) and the nut (5) are also constructed of acrylic. The round construction of the housing (1) was considered in order to provide a large surface around the needle, consisting of uniform thickness and density. This construction exhibits uniform attenuation of the X-ray image such that views of biological contours are not impeded during percutaneous procedures.

A top view of the assembly and a detailed view are presented in Fig. 4b. The needle (6) slides in the hole of the housing (1). Simultaneously, the needle is depressed between the frontal face of the input shaft (2) and the one end of the bushing (3). This axial force is the transmission friction and is implemented loading the O-ring (4) with the nut (5). The O-ring plays here the role of spiral spring. We use an O-ring rather then a metal spring to maintain complete X-ray translucency. The fillet at the base of the frontal face of the shaft (2) was placed in order to diminish the high stress concentration (the week point of the shaft).

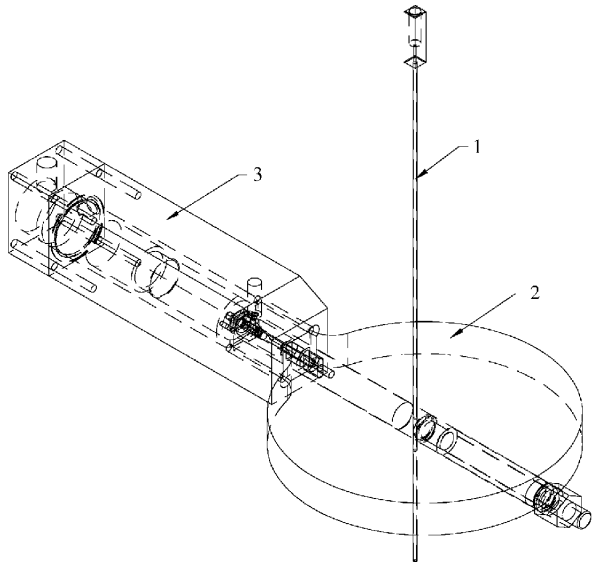

Figure 3. The PAKY assembly

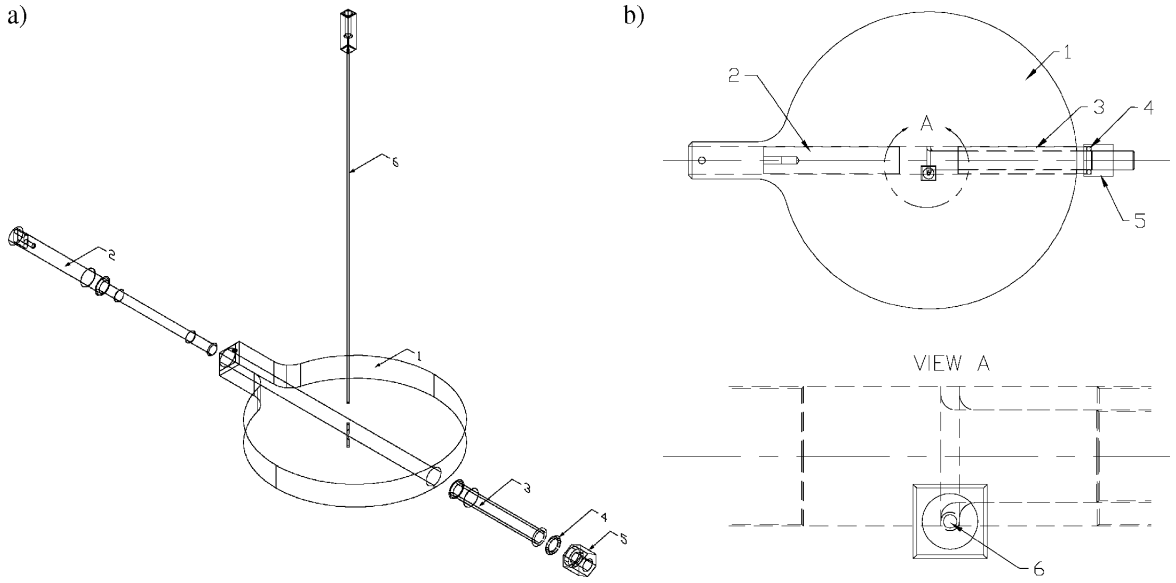

Figure 4. Needle driver: a) Exploded view, b) Top view and detail

As previously mentioned, the transmission slips when overloaded. The overload force is adjustable from the nut (5). With our design we have obtained a drive force of up to 30N for our maximum pre-load tested. The output shaft (needle) was placed as close as possible to the cylindrical face of (2). This resulted into a transmission efficiency of approximately 85%.

4. SYSTEM FOR PERCUTANEOUS ACCESS

We employ a passive arm and the novel needle insertion mechanism, 'PAKY' (Percutaneous Access of the Kidney). The passive (not motorized) arm is a six degree of freedom manipulator (Fig. 5) that may be locked in the desired position. The joints are not equipped with motors or position encoders. A custom designed rigid side rail is mounted on the operating room table to provide a sturdy base for the arm relative to the patient during needle passage. The active injection mechanism,

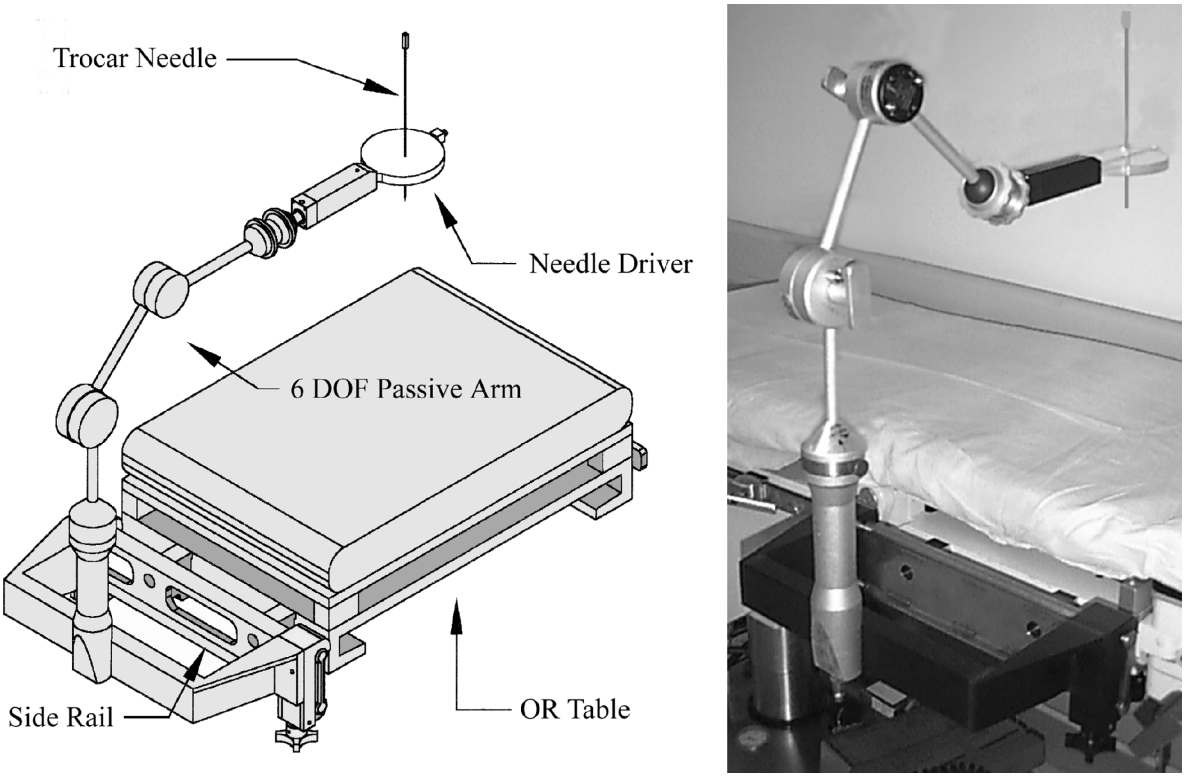

Figure 5. The PAKY system for percutaneous renal access: Schematic and photograph.

PAKY, is attached to the distal end of the arm. As described in the previous section, PAKY is a unique miniaturized radio-lucent construction which provides motorized needle actuation. The needle injection is powered by a DC motor which the surgeon regulates via a proportional joystick.

A variety of materials were assessed balancing radio-lucency versus mechanical strength. The final driver was constructed of acrylic plastic, as it also can be easily sterilized and can be inexpensively manufactured as a disposable unit. A distinctive feature of PAKY is that it grasps the barrel of the needle, not the needle head. This significantly reduces the unsupported length of the needle, thus minimizing the lateral flexure during injection and increasing the accuracy.

4.1. Safety Features:

The PAKY system includes safety features for the patient as well as surgeon. The particular construction of this system reduces the radiation exposure of the surgeon during the registration phase and minimizes it in the needle insertion stage, as compared to similar manual procedures. For both the protection of the surgeon and the patient, the system is powered from batteries, eliminating the risk of exposure to high voltages. Malfunctioning of the electronic components is prevented by using a momentarily-on push-button switch mounted on the joystick that regulates the insertion speed. The variable speed drive allows precise control of the needle insertion. This is extremely effective for compensating the soft tissue deflection, inherent in all biological systems.

The novel friction transmission driving the needle slips when overloaded. This limits the needle insertion force preventing patient injury. The surgeon may choose to adjust this maximum deliverable force by dialing a knob. Furthermore, the system allows to mechanically limit the depth of insertion by choosing the initial elevation of the needle driver with respect to the skin insertion site.

Nevertheless, the injection stage of PAKY is constructed out of plastic, making it inexpensive to manufacture as a sterile, disposable unit. The motor housing and the passive arm that the injector is mounted on are covered with a sterile plastic bag, providing faultless patient protection.

5. IN-VITRO EXPERIMENTS

Experiments to test Pay' s accuracy in needle placement were conducted (see Fig. 6) using a porcine kidney (10 cm long) suspended in agorose gel (1). The accuracy was assessed using a copper ball (2) connected at the end of a wire (3) and the trocar needle (4) as a switch in an electrical circuit (5). The ball was placed into either an upper or lower pole calyx. The needle was targeted, using superimposed registration, at the ball and then inserted. Accurate needle placement was determined by needle-ball contact completing the circuit. Seven balls with diameters varying between 12.5 mm and 3.0 mm were used and the experiment was repeated ten times for each ball.

PAKY is capable of reliably inserting needles at targets as small as 3 mm. It was 100% successful in making needle-ball contact for all 70 attempts. The mechanism proved to be extremely reliable during the experiments and no malfunctions of the mechanical components were encountered.

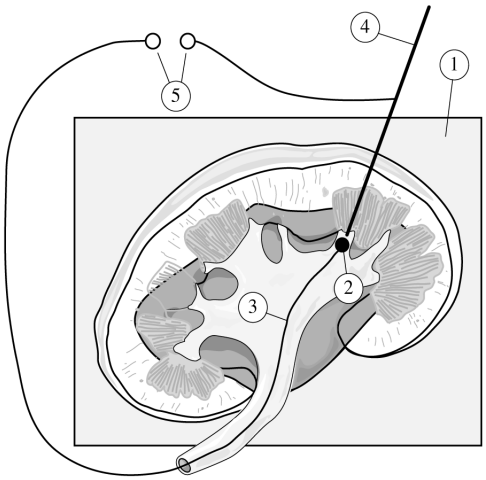

Figure 6. The experiment for needle placement accuracy

6. CONCLUSION

We addressed a particularly difficult surgical task by designing a simple and cost-effective system that could be rapidly transferred to the clinical setting. The advantage of this system for percutaneous renal access is its uncomplicated mimicry of the surgeon's technique while improving both the safety and accuracy of the procedure. The radio-lucent needle driver is fully compatible with, but does *not* require a computer-based vision system or a fully actuated robot with joint position feedback.

REFERENCES

1. Potamianos, P., Davies, B.L., and Hibberd, R.D. Intra-operative imaging guidance for keyhole surgery methodology and calibration. In *Proc. First Int. Symposium on Medical Robotics and Computer Assisted Surgery*, Pittsburgh, PA. p. 98-104, 1994.

2. Potamianos, P., Davies, B.L., and Hibberd, R.D. Intra-operative registration for percutaneous surgery. In *Proc. Second Int. Symposium on Medical Robotics and Computer Assisted Surgery*, Baltimore, MD. p. 156-164, 1995.

3. Bzostek, A., Schreiner, S., Barnes, A.C., Cadeddu, J.A., Roberts, W., Anderson, J.H., Taylor, R.H., Kavoussi, L.R.. An automated system for precise percutaneous access of the renal collecting system. (Submitted for review) *Proceedings the First Joint Conference of CVRMed and MRCAS*, Grenoble, France, 1997.